

SCIENTIFIC REPORTS



OPEN

MRI Assessment of Cardiomyopathy Induced by β 1-Adrenoreceptor Autoantibodies and Protection Through β 3-Adrenoreceptor Overexpression

Received: 26 October 2016
Accepted: 01 February 2017
Published: 09 March 2017

Laetitia Vanhoutte^{1,2}, Céline Guilbaud¹, Ruben Martherus¹, Caroline Bouzin¹, Bernard Gallez³, Chantal Dessy¹, Jean-Luc Balligand¹, Stéphane Moniotte² & Olivier Feron¹

The cardiopathogenic role of autoantibodies (aabs) directed against β 1-adrenoreceptors (β 1-AR) is well established. In mouse models, they cause progressive dilated cardiomyopathy (DCM) whose characterization with echocardiography requires prolonged protocols with numerous animals, complicating the evaluation of new treatments. Here, we report on the characterization of β 1-aabs-induced DCM in mice using 11.7T MRI. C57BL/6J mice ($n = 10$ per group) were immunized against the β 1-AR and left ventricular (LV) systolic function was assessed at 10, 18 and 27 weeks. Increase in LV mass/tibial length ratio was detected as the first modification at 10 weeks together with dilation of cavities, thereby outperforming echocardiography. Significant impairment in diastolic index was also observed in immunized animals before the onset of systolic dysfunction. Morphometric and histological measurements confirmed these observations. The same protocol performed on β 3-AR-overexpressing mice and wild-type littermates ($n = 8-12$ per group) showed that transgenic animals were protected with reduced LV/TL ratio compared to wild-type animals and maintenance of the diastolic index. This study demonstrates that MRI allows a precocious detection of the subtle myocardial dysfunction induced by β 1-aabs and that β 3-AR stimulation blunts the development of β 1-aabs-induced DCM, thereby paving the way for the use of β 3AR-stimulating drugs to treat this autoimmune cardiomyopathy.

Because of its high prevalence, morbidity and mortality, heart failure remains a major health problem. Among the mechanisms leading to this condition, the detrimental role played by autoantibodies targeting the β 1-adrenergic receptor (β 1-aabs) has been established in the last two decades. Clinical studies have shown that the prevalence of β 1-aabs is associated with dilated cardiomyopathy (DCM)¹⁻³, ischemic cardiomyopathy⁴ and Chagas' disease⁵, with – overall – a more frequent occurrence of poor LV function⁴, ventricular arrhythmias⁶, sudden cardiac death^{6,7} and mortality⁸. By contrast, prevalence is apparently lower in patients with heart failure due to valvular or hypertensive diseases⁹. These gross statistics require further clarification in order to better understand the time course of appearance and exact roles of these antibodies in patients suffering from cardiac diseases of various etiologies. A multicentric prospective and retrospective study is currently conducted in patients suffering from myocarditis, ischemic and hypertensive heart diseases¹⁰.

Evidence has accumulated from animal studies confirming the direct pathogenicity of β 1-aabs. A highly antigenic fragment containing B and T cell epitopes has been identified on the second extracellular loop (β 1-EC_{II}) of the β 1-adrenoreceptor (β 1-AR)¹¹⁻¹³. Studies on animal models have established the development of cardiac

¹Pole of Pharmacology and Therapeutics (FATH), Institut de Recherche Expérimentale et Clinique (IREC), Université catholique de Louvain, Brussels, Belgium. ²Department of Paediatric Cardiology, Cliniques universitaires St Luc, Université catholique de Louvain, Brussels, Belgium. ³Biomedical Magnetic Resonance Unit (REMA), Louvain Drug Research Institute (LDRI), Université catholique de Louvain, Brussels, Belgium. Correspondence and requests for materials should be addressed to O.F. (email: olivier.feron@uclouvain.be) or L.V. (email: laetitia.vanhoutte@uclouvain.be)

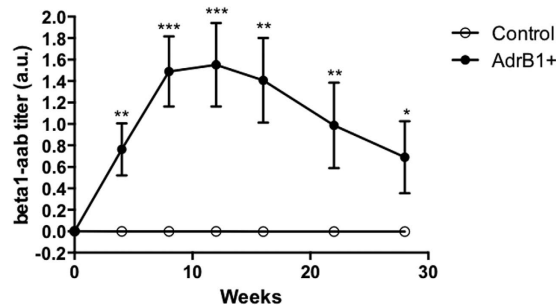


Figure 1. Titer of antibodies against β_1 AR-ECII determined by ELISA throughout the study period, in sera of control (CTL, $n = 10$) and β_1 -immunized (AdrB1+, $n = 7-10$) mice. Data are represented as mean \pm SEM, and normalized to basal optical density obtained before injection, * $P \leq 0.05$; ** $P \leq 0.01$; *** $P \leq 0.001$ vs control.

dysfunction after the active immunization against this antigen (indirect evidence)¹⁴⁻¹⁶ and assessed the possibility of generating cardiac impairment after transfer of homologous pathogenic antibodies to healthy animals (direct evidence)¹⁷. The two main hypotheses raised to explain the development of such antibodies include homologies between the receptor and microbial determinants or the exposition of potentially antigenic components of the cardiomyocytes following cardiac damages¹⁸.

The functional effects of β_1 -aabs at the cellular and molecular levels are incompletely understood. Preliminary results suggest that they act as allosteric agonists¹⁹, enabling dimerization and stabilization of β_1 -AR in its active conformation²⁰, subsequently promoting sustained downstream signaling in a manner distinct from the natural ligand^{21,22}. This leads to cardiomyocyte apoptosis²³, enhanced contractility and prolonged action potential duration²⁴. During progression of aabs-induced cardiomyopathy, increased levels of GRK2 have also been documented in several rodent studies^{16,25,26}, suggesting desensitization and down-regulation of β_1 -AR. Some therapies, including the use of apheresis²⁷, aptamers²⁸, peptides competing with the receptor epitope^{29,30} and conventional beta-blockers^{30,31} have proven to be useful in order to partially prevent the development of cardiac dysfunction due to β_1 -aabs.

The β_3 -adrenoreceptor (β_3 -AR) has recently emerged as a potential therapeutic target in the presence of an excessive β -adrenergic stimulation on the heart, as it mediates a countervailing influence to β_1 and β_2 -AR activation³² and is resistant to homologous desensitization³³. Moreover β_3 -ARs are upregulated under various conditions of adrenergic overstimulation³⁴⁻³⁶, arguing in favor of a potential influence of these receptors on chronic remodeling. Our group has recently demonstrated that transgenic mice with cardiac-specific overexpression of β_3 -AR were protected from hypertrophic and fibrotic remodeling due to neurohormonal stimulation³⁷. Whether β_3 stimulation may prevent or correct autoimmune DCM is however unknown.

Up to now, the anatomical characterization of the cardiomyopathy induced by β_1 -aabs in animals has mostly been performed using echocardiography. However, cardiac dysfunction appears slowly and frequently starts with subtle diastolic dysfunction and elevated filling pressures. With the limited accuracy and reproducibility of echocardiography, prolonged protocols with numerous animals are needed before identifying early modifications in immunized individuals. The recent development of ultra-high field MRI (UHF MRI) has brought new perspectives in cardiovascular imaging of small animal models, due to its higher accuracy and reproducibility³⁸ and the numerous sequences available. Here, we studied the evolution of systolic and diastolic LV function of mice submitted to β_1 -AR immunization with an 11.7T MRI scanner to evaluate whether this technique could permit earlier detection of remodeling induced by aabs. We also aimed to study whether β_3 -AR overexpressing mice could be protected from cardiac remodeling induced by chronic exposure to β_1 -aabs.

Results

Mouse model of β_1 AR aabs-induced cardiomyopathy. We actively immunized C57Bl/6J mice against the β_1 -AR through monthly subcutaneous injections of a peptide corresponding to the second extracellular loop of the receptor, for a total of 28 weeks. In parallel, control animals were s.c. administered the vehicle solution. Immunized mice showed a gradual increase of circulating antibodies directed against β_1 AR-ECII, reaching a peak after 2 booster doses, whereas β_1 -aabs remained undetectable in control mice (Fig. 1). 3 mice died in the immunized group within the first 12 weeks of protocol. Deaths occurred in animals presenting the most rapid increase in antibody titers, suggesting the occurrence of aabs-induced lethal arrhythmias^{39,40}. No alterations in body weight, food intake and behavior were observed in surviving mice.

MRI cardiac function evaluation upon induction of β_1 AR aabs. After 10 weeks of follow-up, mice immunized against the β_1 AR-ECII already showed a statistically significant increase in the LV/TL ratio compared to control mice (4.2 ± 0.1 vs 3.8 ± 0.1 mg/mm, $p < 0.05$) (Fig. 2, left panel and Table 1). Over time, a continuous increase of this parameter was observed in the β_1 -immunized group, accompanied by signs of progressive dilation of LV (Fig. 2, left panel and Table 1). These MRI data for LV mass and LV/TL were confirmed by *ex vivo* measurements at 28 weeks (Table 1).

A statistically significant difference for EDV was noticeable after 18 weeks between treated and control mice (69.1 ± 4.3 vs 59.6 ± 1.5 μ l, $p < 0.05$) (Fig. 2, middle panel and Table 1), and after 27 weeks for ESV (29.0 ± 4.0

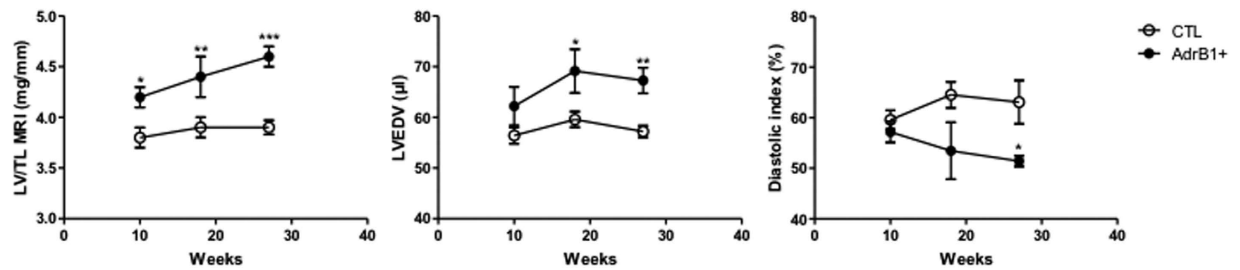


Figure 2. MRI follow-up in β_1 -immunized ($n = 7-9$) and control mice ($n = 10$). The panels depict the time course of the following parameters: LV mass/tibial length ratio (LV/TL), end-diastolic volume (EDV) and diastolic index. Error bars indicate SEM. * $P \leq 0.05$; ** $P \leq 0.01$; *** $P \leq 0.001$; **** $P \leq 0.0001$ vs control.

	10 weeks		18 weeks		27 weeks	
	CTL	AdrB1+	CTL	AdrB1+	CTL	AdrB1+
n	10	9	10	7	10	7
EDV (μl)	56,4 \pm 1,6	64,2 \pm 3,8	59,6 \pm 1,5	69,1 \pm 4,3*	57,2 \pm 1,2	67,3 \pm 2,5**
ESV (μl)	24,0 \pm 2,5	22,9 \pm 2,0	27,0 \pm 13,8	32,0 \pm 14,0	22,0 \pm 1,5	29,0 \pm 4**
SV (μl)	32,6 \pm 2,3	41,4 \pm 3,2*	29,0 \pm 16,3	41,0 \pm 21,0	35,3 \pm 1,0	39,6 \pm 2,6
EF (%)	57,7 \pm 4,0	64,1 \pm 2,7	51,0 \pm 15,5	59 \pm 7,0	61,8 \pm 1,1	58,7 \pm 2,4
LV mass MRI (mg)	74,1 \pm 1,7	81,1 \pm 2,1*	74,8 \pm 1,4	83,9 \pm 3,6*	75,9 \pm 1,1	88,0 \pm 2,0****
LV/TL MRI (mg/mm)	3,8 \pm 0,1	4,2 \pm 0,1*	3,9 \pm 0,1	4,4 \pm 0,2**	3,9 \pm 0,07	4,6 \pm 0,1***
ES septum thickness (mm)	1,5 \pm 0,1	1,3 \pm 0,1	1,2 \pm 0,1	1,4 \pm 0,1	1,4 \pm 0,1	1,4 \pm 0,1
Systolic index (%)	66,8 \pm 1,5	67,8 \pm 2,5	66,8 \pm 1,9	63,2 \pm 3,0	66,5 \pm 1,9	64,8 \pm 2,0
Diastolic index (%)	59,6 \pm 1,9	57,2 \pm 2,1	64,5 \pm 2,6	53,5 \pm 5,6	63,1 \pm 4,3	51,4 \pm 1,1*
LV mass <i>ex vivo</i> (mg)					97,9 \pm 1,9	107,5 \pm 2,7**
LV/TL <i>ex vivo</i> (mg/mm)					5,0 \pm 0,1	5,6 \pm 0,1**

Table 1. *In vivo* MRI parameters in mice at 10, 18 and 27 weeks and *ex vivo* data for LV mass and LV/TL after sacrifice at 28 weeks. n represents the number of animals in each group. EDV = end-diastolic volume; ESV = end-systolic volume; SV = stroke volume; EF = ejection fraction; LV = left ventricle; TL = tibial length; ES = end-systolic. * $P \leq 0.05$; ** $P \leq 0.01$; *** $P \leq 0.001$; **** $P \leq 0.0001$ vs control.

vs $22.0 \pm 1.5 \mu\text{l}$, $p < 0.05$) (Table 1). No difference was observed between the two groups for end-systolic septum thickness. Figure 3 shows representative short-axis images in β_1 -immunized and control mice at the end of the protocol.

Analysis of the diastolic index showed an impaired diastolic function in the treated group from 18 weeks that become significantly altered at 27 weeks (51.4 ± 1.1 vs $63.1 \pm 4.3\%$, $P < 0.05$) (Fig. 2, right panel and Table 1). By contrast, systolic function assessed both by EF and systolic index remained within normal values in the immunized group (Table 1).

Cardiac histology and gene expression upon induction of β_1 AR aabs. Histomorphometric analysis of cardiomyocyte transverse area confirmed significantly larger myocytes with increased vascular density in β_1 -immunized mice ($p < 0.05$) (Fig. 4A). No differences in collagen (Sirius red labeling) (Fig. 4B) or inflammatory infiltration (CD45/CD11b staining) (Fig. 4C and D) were observed between the two groups.

We also performed qPCR analyses to identify changes in mRNA expression from corresponding cardiac tissues (Table 2). mRNA expression of β AR-1 and -2 (ADRB 1–2) remained unchanged between control and β_1 -immunized group while a two-fold increase in β AR-3 gene expression (ADRB3) was observed in the immunized group (although not reaching statistical significance, Table 2). No re-expression of the fetal gene program was found based on the levels of myosin heavy chains (MYH6 and MYH7 coding for the alpha and beta isoform, respectively) and natriuretic peptides (ANP and BNP for atrial and brain forms, respectively); a trend toward an increase in the BNP gene expression was however observed in β_1 -immunized mice ($p = 0.07$, Table 2).

β_3 TG mice are protected from β_1 AR aabs-induced cardiomyopathy. We tested whether the overexpression of the β_3 -AR could protect from developing β_1 -aabs-induced DCM by applying the protocol of immunization previously described to 12 transgenic (heterozygous) mice overexpressing the β_3 -AR (TG) and 12 wild-type littermates (WT). 5 mice died in each group upon active immunization against β_1 AR-EC_{II} before the end of the protocol.

Cardiac MRI measurements after 27 weeks showed statistically significant differences between the two immunized groups: LV/TL ratio remained unaltered in immunized β_3 -overexpressing mice, with a value of

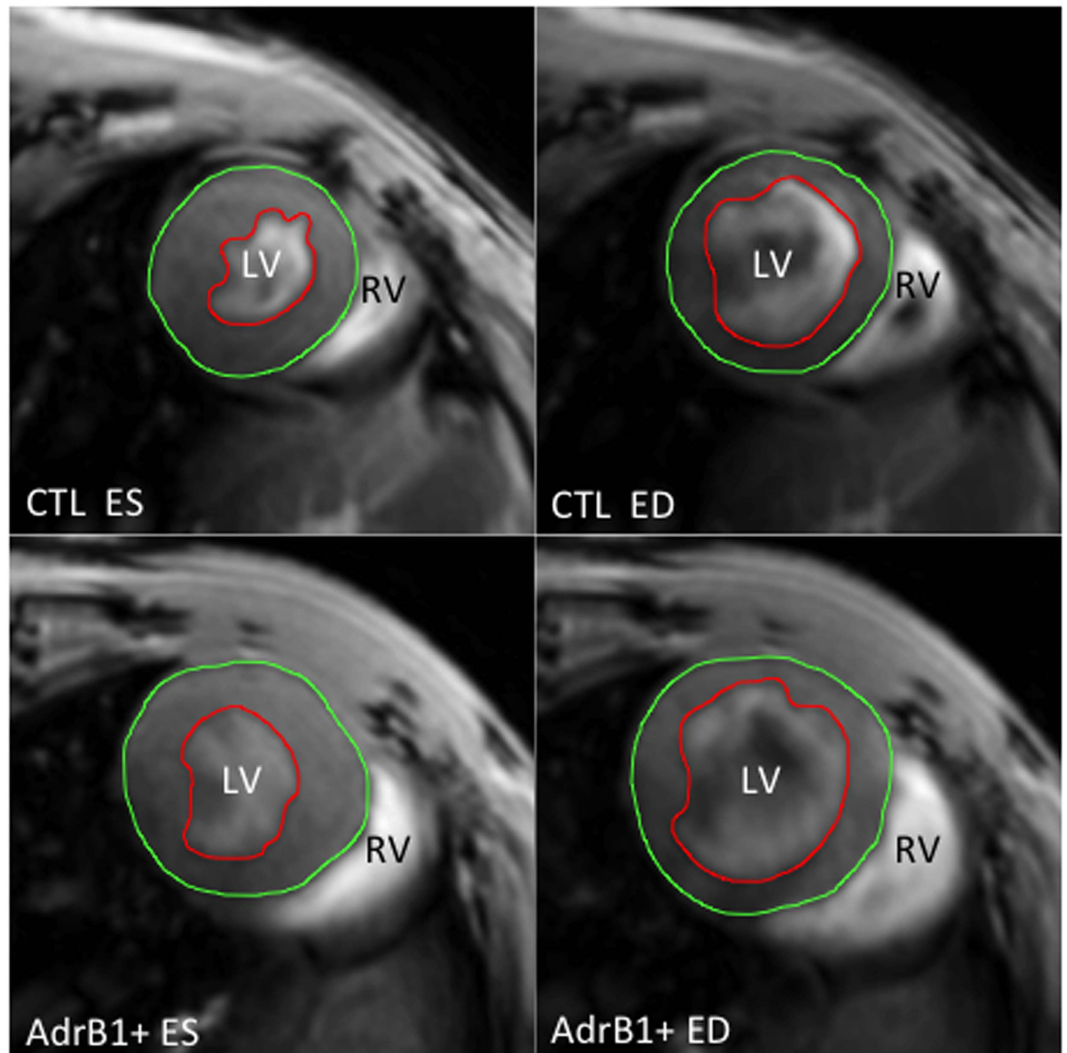


Figure 3. Representative MRI short-axis views of mouse hearts after 27 weeks of evolution in end-diastolic (ED) and end-systolic (ES) phases, with endocardial (red) and epicardial (green) contours, showing left ventricular dilation in β_1 -immunized (AdrB1+) vs control mice. LV = left ventricle, RV = right ventricle.

3.5 ± 0.2 mm/mg (vs. 4.3 ± 0.2 mm/mg in immunized wild-type animals, $p < 0.05$) (Fig. 5A, left panel). These data were confirmed by *ex vivo* LV/TL measurements after sacrifice of the animals (Fig. 5A, right panel). Interestingly, while determination of systolic indexes did not reveal any difference between mouse groups (Fig. 5B), evaluation of diastolic indexes reinforced the concept of β_3 -AR-mediated protection. First, significant differences between the two immunized groups were observed as soon as 18 weeks (Fig. 5C). Second, while LV/TL ratio measurements only revealed a trend towards an increase in control littermates of transgenic animals (see two first sets of points in Fig. 5A graphs), diastolic indexes revealed a statistically significant reduction after 27 weeks, confirming the earliness of diastolic dysfunction in this DCM model (Fig. 5C). Other MRI measurements were not altered when compared to control groups after 27 weeks of follow-up (not shown).

Discussion

The major findings of this study are related to the application of UHF MRI technology to study the early development of β_1 aabs-driven autoimmune cardiac dysfunction and to the identification of β_3 -AR as key actor of a counterbalancing pathway preventing the occurrence of DCM in this model.

Previous studies using echocardiography have reported the first anatomical changes at rest in β_1 -immunized BalbC²⁵ and C57BL/6J mice²⁶ at 25 weeks. In our study with C57BL/6J mice immunized against the β_1 -AR, using UHF MRI, we were able to show early aabs-induced cardiomyopathic changes after only 10 weeks. LV hypertrophy (increase in LV/TL ratio) was detected before transition to the complete phenotype of DCM. Furthermore, we applied to our UHF MRI study a recently described method based on the concepts of echocardiographic color kinesis^{41,42} in order to derive systolic and diastolic indexes in our animals. This led us to document that diastolic dysfunction was detectable before the occurrence of systolic dysfunction. These results open new perspectives for clinical investigations in patients carrying β_1 -aabs. Indeed, several methods (i.e. echographic speckle tracking and MR tagging ref. 43) are now available besides the classical echocardiographic mitral inflow color Doppler

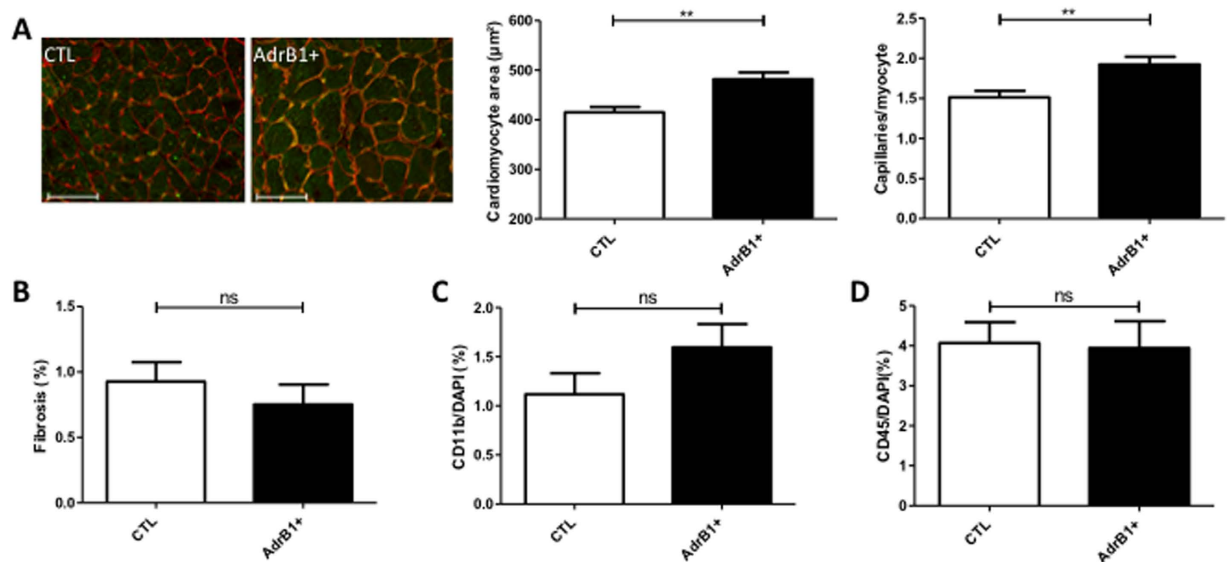


Figure 4. Histology of mouse hearts. (A) Left panel: representative cross-sections of hearts from control and $\beta 1$ -immunized (AdrB1+) mice stained with isolectin B4 (green) and wheat germ agglutinin (red). Scale bar, 50 μm . Right panel: columns indicate the respective myocyte area and capillary density from same sections in each group, showing cardiomyocyte hypertrophy compensated by higher capillary density in hearts from immunized mice. (B) Quantification of collagen infiltration with sirius red staining. (C,D) Quantification of inflammatory infiltration with CD11b and CD45 stainings. * $P \leq 0.05$; ** $P \leq 0.01$ vs control. $n = 7-10$ mice per group.

Gene	Control mice	Immunized mice	p-value
ADRB1	1.00 \pm 0.07	0.98 \pm 0.10	0,87 (ns)
ADRB2	1.00 \pm 0.07	0.94 \pm 0.07	0,60 (ns)
ADRB3	1.00 \pm 0.30	2.02 \pm 0.39	0,11 (ns)
MYH6	1.00 \pm 0.34	1.56 \pm 0.58	0,39 (ns)
MYH7	1.00 \pm 0.31	0.64 \pm 0.26	0,40 (ns)
ANP	1.00 \pm 0.19	1.14 \pm 0.24	0,65 (ns)
BNP	1.00 \pm 0.11	1.83 \pm 0.46	0,07 (ns)

Table 2. mRNA expressions in heart lysates after 28 weeks of treatment. Data are presented as mean \pm SEM, mRNA expressions in $\beta 1$ -immunized mice ($n = 7$) are normalized to expression measured in control mice ($n = 10$).

(E/A) measurements in order to thoroughly investigate diastolic function in patients. If these data are confirmed by further clinical studies, appearance of diastolic dysfunction in $\beta 1$ -aabs-positive patients could be used as an early marker of evolution to heart failure, requiring an intensification of treatments.

Besides the above technological benefits of UHF MRI applied to autoimmune DCM, we showed that transgenic mice harboring a cardiac-specific human $\beta 3$ -AR transgene were protected from myocardial dysfunction induced by $\beta 1$ -aabs. Although, unlike in C57BL/6J mice, only a trend to a cardiac dilation (ie, increased LV/TL ratio) was detectable in the immunized WT group (vs. non-immunized mice) at the end of our study, a significant reduction in the diastolic index confirmed the development of $\beta 1$ aabs-mediated cardiac alterations in these mice. Different genetic backgrounds are likely to account for the LV/TL ratio discrepancy but this observation also emphasize the earliness of the diastolic dysfunction in this model of autoimmune DCM. Importantly, in $\beta 3$ -AR overexpressing mice, the diastolic index was not decreased in response to immunization and was actually even slightly increased. Altogether, these data indicate a significant protective effect of $\beta 3$ -AR overexpression against the development of heart damage induced by $\beta 1$ -aabs (vs. immunized WT mice) and thereby open new therapeutic perspectives in the treatment of autoimmune DCM.

As $\beta 3$ -AR have functionally opposite effects to $\beta 1$ -AR and $\beta 2$ -AR on cardiac muscle and are more resistant than $\beta 1$ -AR and $\beta 2$ -AR to homologous desensitization³³, they represent attractive candidates for efficient pharmacological modulation in the diseased heart⁴⁴. Recent data published by our team have already shown that $\beta 3$ TG mice were protected against early cardiac dysfunction induced by neurohormone infusion (i.e. angiotensin II or isoproterenol)³⁷. The present study confirms the potential beneficial effects of $\beta 3$ -adrenergic stimulation to also prevent the development of autoimmune DCM. In addition to the attenuation of $\beta 1$ -adrenergic inotropic responses, the nitric oxide production consecutive to a $\beta 3$ -AR stimulation of microvascular endothelial cells⁴⁵ and cardiac myocytes³⁷ may help to maintain a normal left ventricular diastolic function during the early stages

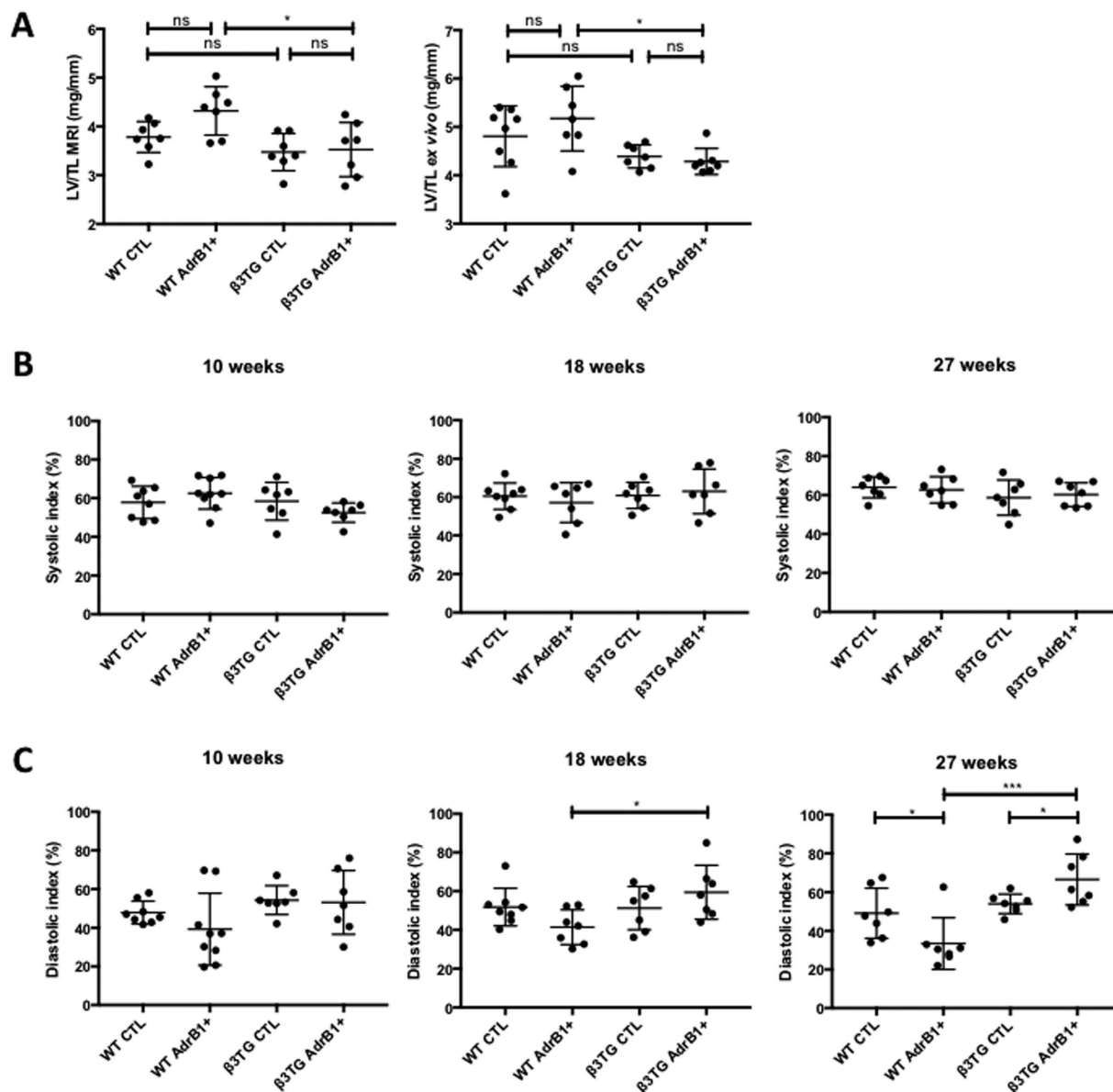


Figure 5. (A) MRI LV/TL (left) and *ex vivo* LV/TL (right) ratios at 27 and 28 weeks, respectively, in transgenic mice overexpressing the beta3 adrenergic receptor and immunized (TG AdrB1+) or not (TG CTL) against AdrB1-ECII, and their wild-type littermates with (WT AdrB1+) or without (WT CTL) immunization. Systolic (B) and diastolic (C) indexes determined in the same animals after 10, 18 and 27 weeks, * $P \leq 0.05$; ** $P \leq 0.01$ as indicated.

of cardiac dysfunction; improving diastolic relaxation can indeed exert a beneficial hemodynamic effect through the maintenance of the Frank-Starling response⁴⁶. The latter property seems even more relevant for the treatment of β1-aabs-induced cardiomyopathy, in the light of the early diastolic dysfunction reported in mice immunized against β1-ECII.

A limitation in our study is the use of transgenic β3 AR-overexpressing mice which *per se* means that this pathway is continuously influencing the cardiac phenotype of these animals and may thus prevent dysfunction from the earliest stages of its development. Still, these results pave the way for the evaluation of *bona fide* β3-AR agonists or the preferred use of β-blockers endowed with such β3-AR stimulatory activity in the treatment of autoimmune β1-aabs-induced DCM. Nebivolol represents a third generation selective β1-AR antagonist with ancillary metabolic effects involving a β3-AR stimulation. Nebivolol could thus bring an increment of efficacy *vs.* conventional beta-blockers whose usefulness has already been demonstrated in the context of β1-aabs-induced DCM (with however a lower efficiency than therapies using neutralizing peptides)³⁰. We previously showed that nebivolol treatment of coronary microvessels led to NO-dependent vasorelaxation⁴⁷ while others documented a further protection of nebivolol administration against endothelial dysfunction through a net reduction in oxidative stress⁴⁸. Altogether these studies suggest that the dual β1/β3-AR modulation, already demonstrated in

previous studies for heart failure and myocardial infarction with Nebivolol⁴⁹, could be extended to patients with β_1 -aabs-induced DCM.

In conclusion, we showed that UHF MRI allows the precocious detection of mouse myocardial remodeling induced by β_1 -aabs, at earlier time-points than anticipated based on previous reports using echocardiography. Importantly, this technology allowed us to identify a diastolic dysfunction occurring before the onset of systolic dysfunction in this autoimmune cardiac disease and to provide evidence supporting the therapeutic potential of drugs endowed with beta-3 AR agonistic activity for the treatment of β_1 -aabs-induced DCM.

Methods

Animals and immunization. All the experiments involving mice received the approval of the “Comité d’Ethique pour l’Expérimentation Animale de l’Université catholique de Louvain” (approval reference #2012/UCL/MD005) and were carried out according to national animal care regulations. This study conforms to the Guide for the Care and Use of Laboratory Animals published by the US National Institutes of Health (NIH Publication No. 85–23, revised 1996). Mice were housed under standard conditions with *ad libitum* access to water and chow.

C57BL/6J mice. A group of ten 8-weeks C57BL/6J male mice (Janvier, Paris, France) were monthly immunized with 200 μ g of a synthetic peptide (Eurogentec, Seraing, Belgium) corresponding to the human and mouse β_1 AR-EC_{II} (residues 197–222: H-W-W-R-A-E-S-D-E-A-R-R-C-Y-N-D-P-K-C-C-D-F-V-T-N-R) through subcutaneous injection. The peptide was dissolved in 0.1 M Na₂CO₃/1% β -mercaptoethanol and emulsified in complete Freund’s adjuvant for the first injection and incomplete adjuvant for the followings in order to avoid excessive inflammatory response. Another group of 10 C57BL/6J male mice received only the vehicle and were used as controls. Mice were anaesthetized (150 mg/kg ketamine, 10 mg/kg xylazine, i.p.) prior each injection, allowing simultaneous collection of retro-orbital blood samples.

β 3TG mice. Male mice harboring an α -myosin heavy chain promoter-driven human β_3 -AR transgene generated as described previously⁵⁰, were used to produce heterozygous β 3TG mice and wild-type littermate controls (n = 40); the original β 3TG mouse line had been selected to exhibit a moderate overexpression of the transgene (matching the *ex vivo* myocardial response to a β_3 -AR agonist). Mice from β 3TG and wild-type groups were randomly distributed in two subgroups and immunized according to the protocol described above, except that subcutaneous injections were performed under light anaesthesia with isoflurane 2–3% in oxygen for 3 minutes, and that no retro-orbital blood sample was taken at the same time to minimize animal stress. 12 mice per group were immunized with the peptide while 8 mice per group receive the vehicle and were used as controls.

Morphometric measurements. At the end of the study, after a follow-up of 28 weeks, animals were euthanized by cervical dislocation and their left ventricular weight and tibial length were measured. Hearts and sera were collected for analysis and stored at -80°C .

Autoantibody detection. To detect β_1 AR autoantibodies in mouse sera, the β_1 AR-EC_{II} synthetic peptide was used in an enzyme-linked immunosorbent assay (ELISA). Plates (Reacti-Bind, Thermo scientific, Rockford, IL) were coated overnight at room temperature with 1 μ g/ml peptide (Eurogentec, Seraing, Belgium). Coating and blocking procedures were carried out using Ultrablock and Neptune buffers from AbD Serotec (Oxford, UK) according to the manufacturer’s instructions. Sera (diluted 1/2500) were then incubated overnight at 4°C . After washing, specific hybridization was measured with a peroxidase-conjugated antimouse IgG antibody (dilution 1/10000) and addition of 3,3',5,5'-tetramethylbenzidine from Calbiochem (Merck Chemicals, Nottingham, UK). The absorbance was determined at 450 nm in a microplate reader (Victor X4; Perkin Elmer, Waltham, MA).

MRI measurements. **Cardiac MRI (CMR) acquisition.** Each animal was scanned at 10, 18 and 27 weeks of treatment on a 11.7T MRI scanner dedicated to small animal applications (Biospec, Bruker, Ettlingen, Germany). A quadrature ¹H resonator was used for radiofrequency transmission (inner diameter = 72 mm, length = 6.6 cm) in conjunction with a surface receive-only coil array (length = 10.7 cm). Anaesthesia was induced with 3% isoflurane in oxygen, and then maintained with 0.5–2% isoflurane during the entire procedure, in order to remain within physiological heart rates (around 500 heartbeats/min). Animals were placed in prone position and monitored for electrocardiogram and respiration with neonatal electrodes wrapped around the paws and a pneumatic sensor placed under the animal. The body temperature was followed by using a rectal probe and regulated with a dedicated heating blanket. Cardiac scout images were obtained in the conventional planes with a tripilot sequence. Then an IntraGate 2D cine Fast Low Angle Shot (FLASH) sequence was applied to acquire a stack of seven to eight 1-mm thick contiguous short-axis images covering the entire ventricles, perpendicular to the LV long-axis. Imaging parameters: repetition time: 5.83 ms; echo time: 1.45 ms; flip angle: 25° ; field of view: 30.0×30.0 ; and matrix size: 256×256 ; resulting in an in-plane resolution of $0.12 \times 0.12 \text{ mm}^2$.

CMR Image analysis. The LV systolic function was assessed from the stack of short axis images by tracing epicardial and endocardial borders on Segment software (Medviso v1.8, Lund, Sweden). End-diastolic (EDV), end-systolic (ESV) and stroke volume (SV) were determined (μ l). LV ejection fraction (EF, as %) and LV mass (mg) were subsequently deduced. Systolic and diastolic indexes were determined as previously described^{41,42}. Briefly, we visually determined the end-diastolic phase, end-systolic phase and the phase at 30% of diastole, and traced the endocardial contours at the mid-ventricular level on the Osirix imaging software (v4.0; Pixmeo; Geneva, Switzerland). Then we calculated the systolic fractional area change (systolic index, as %) through the following formula: EDA-ESA/EDA , where EDA = end-diastolic area and ESA = end-systolic area. The fractional

area change during the first 30% of diastole (diastolic index, as %) was also calculated through the following formula: $dA\text{-ESA}/EDA\text{-ESA}$, where dA = area at 30% of diastole. All analyses were performed on a blinded basis.

Cardiac histochemistry. At the end of the study hearts were excised and representative pieces of left ventricles were fixed in 4% formaldehyde after rinsing with saline. For analysis of cardiac fibrosis, 5- μm sections of paraffin embedded hearts were stained with picrosirius red. Stained sections were digitalized with a SCN400 slide scanner (Leica Biosystems, Wetzlar, Germany). Quantification was made with Tissue IA software (Leica Biosystems, Dublin, Ireland). Area occupied by interstitial fibrosis was expressed as a percentage of total myocardial area. To quantify transverse cardiomyocyte area and capillary density, cryosections were stained with Wheat germ agglutinin (WGA) as a membrane marker, and with biotinylated-Isolectine B4 as an endothelial marker. Mounted slides were observed with an Axioimager Z1/Apoptome microscope equipped with a MRM camera (Zeiss, Germany). The data analysis was performed with Axiovision software (Zeiss, Germany). A minimum of 40 to 100 cells from 9 sections were measured in each heart. Other heart cryosections were incubated with antibodies raised against the monocyte marker CD11b and the lymphocytic marker CD45 (rat anti-CD11b and rat anti-CD45, both from BD Bioscience, San Jose, CA). Slides were scanned with a MIRAX Scanner (Zeiss, Germany) and analyzed with FRIDA software (Johns Hopkins University, Baltimore, MD). All analyses were performed on a blinded basis.

Quantitative Polymerase Chain Reaction (qPCR). Total RNA was isolated from heart tissues using TRI-reagent (Fermentas, Alost, Belgium) according to the manufacturer's instructions. 1 μg total RNA was reverse transcribed with RevertAidTM M-MuLV Reverse Transcriptase (ThermoFischer Scientific, Alost, Belgium) using hexamer primers. Resulting cDNA served as template for quantitative real-time PCR analysis using the following primers: *Adrb1* (Forward: 5'-GCTGATCTGGTCATGGGATT-3', Reverse: 5'-AAGTCCAGAGCTCGCAGAAG-3'), *Adrb2* (Forward: 5'-TTCGAAAACCTATGGGAACG-3', Reverse: 5'-GGGATCCTCACACAGCAGTT-3'), *Adrb3* (Forward: 5'-ACCAGAAGCCCTCAGCATCCCA-3', Reverse: 5'-CACCCGCTTGTTCAGGAGTAC-3'), *Myh6* (Forward: 5'-GGGACATTGGTGCCAAGAAGA-3', Reverse: 5'-ATTGTGGATTGGCCACAGCG-3'), *Myh7* (Forward: 5'-ACCAACCTGTCCAAGTTCCG-3', Reverse: 5'-ACTCCTCATTGAGCCCTTG-3'), *Nppa* (Forward: 5'TGATAGATGAAGGCAGGAAGCCGC-3', Reverse: 5'-AGGATTGGAGCCAGAGTGGACTAGG-3'), *Nppb* (Forward: 5'-GCCAGTCTCCAGAGC AATTC-3', Reverse: 5'-AGCTGTCTCTGGGCCATTT-3'), *Gapdh* (Forward: 5'-TGCACCACCAACTGCTTAGC-3', Reverse: 5'-GGATGCAGGGATGATGTTCT-3'). All samples were processed in triplicate reactions using Takyon for SYBR low Rox (Eurogentec, Seraing, Belgium) on the ViiA7 Real-Time PCR System (Applied Biosystems) using a fast cycling protocol. GAPDH was used as a reference endogenous gene to normalize the results. Results are shown as fold expression relative to untreated samples according to the $\Delta\Delta C_T$ method.

Statistical Analysis. Data are expressed as mean \pm SEM. Raw data were analyzed for normal distribution using the Shapiro-Wilk test. When normally distributed, unpaired Student *t* test was used to compare differences between two groups and one-way analysis of variance followed by Bonferroni post-hoc test was used to compare 3 or more groups. In the absence of normal distribution, the statistical significance of differences was tested with non-parametric tests (Mann-Whitney or Kruskal-Wallis followed by Dunn's test). $P < 0.05$ was considered statistically significant. Statistical analyses were performed with GraphPad Prism 5.04 (San Diego, CA) and JMP 11.2.0 (SAS Institute, Cary, NC).

References

1. Limas, C. J., Goldenberg, I. F. & Limas, C. Assessment of immune modulation of beta-adrenergic pathways in human dilated cardiomyopathy: influence of methodologic factors. *Am Heart J* **123**, 967–970 (1992).
2. Magnusson, Y., Wallukat, G., Waagstein, F., Hjalmarson, A. & Hoebcke, J. Autoimmunity in idiopathic dilated cardiomyopathy. Characterization of antibodies against the beta 1-adrenoceptor with positive chronotropic effect. *Circulation* **89**, 2760–2767 (1994).
3. Wallukat, G., Wollenberger, A., Morwinski, R. & Pitschner, H. F. Anti-beta 1-adrenoceptor autoantibodies with chronotropic activity from the serum of patients with dilated cardiomyopathy: mapping of epitopes in the first and second extracellular loops. *J Mol Cell Cardiol* **27**, 397–406 (1995).
4. Jahns, R. *et al.* Autoantibodies activating human beta1-adrenergic receptors are associated with reduced cardiac function in chronic heart failure. *Circulation* **99**, 649–654 (1999).
5. Elies, R. *et al.* Structural and functional analysis of the B cell epitopes recognized by anti-receptor autoantibodies in patients with Chagas' disease. *J Immunol* **157**, 4203–4211 (1996).
6. Bohl, S. *et al.* Advanced methods for quantification of infarct size in mice using three-dimensional high-field late gadolinium enhancement MRI. *Am J Physiol Heart Circ Physiol* **296**, H1200–1208 (2009).
7. Iwata, M. *et al.* Autoantibodies against the second extracellular loop of beta1-adrenergic receptors predict ventricular tachycardia and sudden death in patients with idiopathic dilated cardiomyopathy. *J Am Coll Cardiol* **37**, 418–424 (2001).
8. Stork, S. *et al.* Stimulating autoantibodies directed against the cardiac beta1-adrenergic receptor predict increased mortality in idiopathic cardiomyopathy. *Am Heart J* **152**, 697–704 (2006).
9. Jahns, R. *et al.* Activating beta-1-adrenoceptor antibodies are not associated with cardiomyopathies secondary to valvular or hypertensive heart disease. *J Am Coll Cardiol* **34**, 1545–1551 (1999).
10. Deubner, N. *et al.* Cardiac beta1-adrenoceptor autoantibodies in human heart disease: rationale and design of the Etiology, Titre-Course, and Survival (ETICS) Study. *Eur J Heart Fail* **12**, 753–762 (2010).
11. Magnusson, Y. *et al.* Antigenic analysis of the second extra-cellular loop of the human beta-adrenergic receptors. *Clin Exp Immunol* **78**, 42–48 (1989).
12. Tate, K. *et al.* Epitope analysis of T- and B-cell response against the human beta 1-adrenoceptor. *Biochimie* **76**, 159–164 (1994).
13. Mobini, R. *et al.* Probing the immunological properties of the extracellular domains of the human beta(1)-adrenoceptor. *J Autoimmun* **13**, 179–186 (1999).
14. Matsui, S. *et al.* Peptides derived from cardiovascular G-protein-coupled receptors induce morphological cardiomyopathic changes in immunized rabbits. *J Mol Cell Cardiol* **29**, 641–655 (1997).

15. Iwata, M. *et al.* Autoimmunity against the second extracellular loop of beta(1)-adrenergic receptors induces beta-adrenergic receptor desensitization and myocardial hypertrophy *in vivo*. *Circ Res* **88**, 578–586 (2001).
16. Buvall, L., Bollano, E., Chen, J., Shultze, W. & Fu, M. Phenotype of early cardiomyopathic changes induced by active immunization of rats with a synthetic peptide corresponding to the second extracellular loop of the human beta-adrenergic receptor. *Clin Exp Immunol* **143**, 209–215 (2006).
17. Jahns, R. *et al.* Direct evidence for a beta 1-adrenergic receptor-directed autoimmune attack as a cause of idiopathic dilated cardiomyopathy. *J Clin Invest* **113**, 1419–1429 (2004).
18. Jahns, R., Boivin, V. & Lohse, M. J. beta(1)-Adrenergic receptor function, autoimmunity, and pathogenesis of dilated cardiomyopathy. *Trends Cardiovasc Med* **16**, 20–24 (2006).
19. Jahns, R., Boivin, V. & Lohse, M. J. Beta 1-adrenergic receptor-directed autoimmunity as a cause of dilated cardiomyopathy in rats. *Int J Cardiol* **112**, 7–14 (2006).
20. Gouldson, P. R. *et al.* Dimerization and domain swapping in G-protein-coupled receptors: a computational study. *Neuropsychopharmacology* **23**, S60–77 (2000).
21. Tutor, A. S., Penela, P. & Mayor, F. Jr. Anti-beta1-adrenergic receptor autoantibodies are potent stimulators of the ERK1/2 pathway in cardiac cells. *Cardiovasc Res* **76**, 51–60 (2007).
22. Hebert, T. E. Anti-beta1AR antibodies in dilated cardiomyopathy: are these a new class of receptor agonists? *Cardiovasc Res* **76**, 5–7 (2007).
23. Staudt, Y. *et al.* Beta1-adrenoceptor antibodies induce apoptosis in adult isolated cardiomyocytes. *Eur J Pharmacol* **466**, 1–6 (2003).
24. Christ, T. *et al.* Autoantibodies against the beta1 adrenoceptor from patients with dilated cardiomyopathy prolong action potential duration and enhance contractility in isolated cardiomyocytes. *J Mol Cell Cardiol* **33**, 1515–1525 (2001).
25. Buvall, L., Tang, M. S., Isic, A., Andersson, B. & Fu, M. Antibodies against the beta1-adrenergic receptor induce progressive development of cardiomyopathy. *J Mol Cell Cardiol* **42**, 1001–1007 (2007).
26. Ma, L. P., Premaratne, G., Bollano, E., Lindholm, C. & Fu, M. Interleukin-6-deficient mice resist development of experimental autoimmune cardiomyopathy induced by immunization of beta1-adrenergic receptor. *Int J Cardiol* **155**, 20–25 (2012).
27. Matsui, S. *et al.* Specific removal of beta1-adrenoceptor autoantibodies by immunoabsorption in rabbits with autoimmune cardiomyopathy improved cardiac structure and function. *J Mol Cell Cardiol* **41**, 78–85 (2006).
28. Haberland, A., Wallukat, G., Dahmen, C., Kage, A. & Schimke, I. Aptamer neutralization of beta1-adrenoceptor autoantibodies isolated from patients with cardiomyopathies. *Circ Res* **109**, 986–992 (2011).
29. Munch, G. *et al.* Administration of the cyclic peptide COR-1 in humans (phase I study): *ex vivo* measurements of anti-beta1-adrenergic receptor antibody neutralization and of immune parameters. *Eur J Heart Fail* **14**, 1230–1239 (2012).
30. Boivin, V. *et al.* Novel receptor-derived cyclopeptides to treat heart failure caused by anti-beta1-adrenoceptor antibodies in a human-analogous rat model. *PLoS One* **10**, e0117589 (2015).
31. Miao, G. B. *et al.* Autoantibody against beta1-adrenergic receptor and left ventricular remodeling changes in response to metoprolol treatment. *Eur J Clin Invest* **36**, 614–620 (2006).
32. Niu, X. *et al.* Cardioprotective effect of beta-3 adrenergic receptor agonism: role of neuronal nitric oxide synthase. *J Am Coll Cardiol* **59**, 1979–1987 (2012).
33. Liggett, S. B., Freedman, N. J., Schwinn, D. A. & Lefkowitz, R. J. Structural basis for receptor subtype-specific regulation revealed by a chimeric beta 3/beta 2-adrenergic receptor. *Proc Natl Acad Sci USA* **90**, 3665–3669 (1993).
34. Moniotte, S. *et al.* Upregulation of beta(3)-adrenoceptors and altered contractile response to inotropic amines in human failing myocardium. *Circulation* **103**, 1649–1655 (2001).
35. Dincer, U. D. *et al.* The effect of diabetes on expression of beta1-, beta2-, and beta3-adrenoceptors in rat hearts. *Diabetes* **50**, 455–461 (2001).
36. Moniotte, S. *et al.* Sepsis is associated with an upregulation of functional beta3 adrenoceptors in the myocardium. *Eur J Heart Fail* **9**, 1163–1171 (2007).
37. Belge, C. *et al.* Enhanced expression of beta3-adrenoceptors in cardiac myocytes attenuates neurohormone-induced hypertrophic remodeling through nitric oxide synthase. *Circulation* **129**, 451–462 (2014).
38. Vanhoutte, L. *et al.* Variability of Mouse Left Ventricular Function Assessment by 11.7 Tesla MRI. *J Cardiovasc Transl Res* (2015).
39. Lee, H. C., Huang, K. T., Wang, X. L. & Shen, W. K. Autoantibodies and cardiac arrhythmias. *Heart Rhythm* **8**, 1788–1795 (2011).
40. Zuo, L. *et al.* Pro-arrhythmic action of autoantibodies against the second extracellular loop of beta1-adrenoceptor and its underlying molecular mechanisms. *Int J Cardiol* **198**, 251–258 (2015).
41. Okayama, S. *et al.* Evaluation of left ventricular diastolic function by fractional area change using cine cardiovascular magnetic resonance: a feasibility study. *J Cardiovasc Magn Reson* **15**, 87 (2013).
42. Buonincontri, G., Hu, C.-H., Sawiak, S. & Krieg, T. *P516Diastolic dysfunction in diabetic mice revealed by MR* (2014).
43. Daneshvar, D. *et al.* Diastolic dysfunction: improved understanding using emerging imaging techniques. *Am Heart J* **160**, 394–404 (2010).
44. Balligand, J. L. beta(3)-Adrenoceptor stimulation on top of beta(1)-adrenoceptor blockade “Stop or Encore?”. *J Am Coll Cardiol* **53**, 1539–1542 (2009).
45. Dessy, C. *et al.* Endothelial beta3-adrenoceptors mediate vasorelaxation of human coronary microarteries through nitric oxide and endothelium-dependent hyperpolarization. *Circulation* **110**, 948–954 (2004).
46. Heymes, C., Vanderheyden, M., Bronzwaer, J. G., Shah, A. M. & Paulus, W. J. Endomyocardial nitric oxide synthase and left ventricular preload reserve in dilated cardiomyopathy. *Circulation* **99**, 3009–3016 (1999).
47. Dessy, C. *et al.* Endothelial beta3-adrenoceptors mediate nitric oxide-dependent vasorelaxation of coronary microvessels in response to the third-generation beta-blocker nebivolol. *Circulation* **112**, 1198–1205 (2005).
48. Mason, R. P., Kalinowski, L., Jacob, R. F., Jacoby, A. M. & Malinski, T. Nebivolol reduces nitroxidative stress and restores nitric oxide bioavailability in endothelium of black Americans. *Circulation* **112**, 3795–3801 (2005).
49. Sorrentino, S. A. *et al.* Nebivolol exerts beneficial effects on endothelial function, early endothelial progenitor cells, myocardial neovascularization, and left ventricular dysfunction early after myocardial infarction beyond conventional beta1-blockade. *J Am Coll Cardiol* **57**, 601–611 (2011).
50. Tavernier, G. *et al.* beta3-Adrenergic stimulation produces a decrease of cardiac contractility *ex vivo* in mice overexpressing the human beta3-adrenergic receptor. *Cardiovasc Res* **59**, 288–296 (2003).

Acknowledgements

The authors wish to thank the Biomedical Magnetic Resonance Unit (REMA) for assistance during MRI manipulations. We thank Chantal Fregimilicka (IREC Imaging Platform - 2IP) for histochemistry experiments and Sabrina El Bachiri (technological platform for Methodology Support and Statistical Calculation - SMCS) for helpful discussions about statistical analysis. This work was supported by grants from the Fonds de la Recherche Scientifique FRS-FNRS, the Foundation Saint-Luc and the National Foundation for Research in Pediatric Cardiology. LV, CD and OF are Research Fellow, Senior Research Associate and honorary Research Director of the FRS-FNRS, respectively.

Author Contributions

O.F. and C.D. conceived and designed the immunization experiments. L.V.H., S.M. and J.L.B. conceived and analysed the cardiac M.R.I. experiments. L.V.H. performed the experiments including all the MRI-related measurements under the supervision of B.G. and S.M., C.G. and L.V.H. handled the animals for blood and tissue collection. R.M. and C.B. supervised qPCR and histological experiments, respectively. L.V.H. and O.F. prepared figures and L.V.H., S.M. and O.F. wrote the manuscript. All authors reviewed the manuscript.

Additional Information

Competing Interests: The authors declare no competing financial interests.

How to cite this article: Vanhoutte, L. *et al.* MRI Assessment of Cardiomyopathy Induced by β 1-Adrenoreceptor Autoantibodies and Protection Through β 3-Adrenoreceptor Overexpression. *Sci. Rep.* **7**, 43951; doi: 10.1038/srep43951 (2017).

Publisher's note: Springer Nature remains neutral with regard to jurisdictional claims in published maps and institutional affiliations.



This work is licensed under a Creative Commons Attribution 4.0 International License. The images or other third party material in this article are included in the article's Creative Commons license, unless indicated otherwise in the credit line; if the material is not included under the Creative Commons license, users will need to obtain permission from the license holder to reproduce the material. To view a copy of this license, visit <http://creativecommons.org/licenses/by/4.0/>

© The Author(s) 2017